Science Advances
AAAS

advances.sciencemag.org/cgi/content/full/6/6/eaax0947/DC1

Supplementary Materials for

Stochastic transcriptional pulses orchestrate flagellar biosynthesis in *Escherichia coli*

J. Mark Kim, Mayra Garcia-Alcala, Enrique Balleza, Philippe Cluzel*

*Corresponding author. Email: cluzel@mcb.harvard.edu

Published 5 February 2020, *Sci. Adv.* **6**, eaax0947 (2020)
DOI: 10.1126/sciadv.aax0947

This PDF file includes:

SUPPLEMENTAL STRAIN CONSTRUCTION METHODS

a. "Scarless" Chromosomal Engineering

To generate point-mutations or insert sequences without selective markers, we used a "scarless" chromosomal engineering technique—i.e. a genome editing strategy that eliminates extraneous sequences such as antibiotic resistance cassettes (*50*). We modified a dual selection/counter-selection cassette in pKD45 (*51*) consisting of a kanamycin resistance marker and a toxin ccdB driven by a rhamnose inducible promoter (P_{RhaB}). This original cassette required counter-selection to be done on minimal M9 plates containing rhamnose because presence of other carbon sources allowed cells to avoid activation of the rhamnose promoter and escape counter selection. Cell growth was extremely slow on these plates, requiring almost two full days of incubation before colonies became visible. To overcome this limitation, we replaced the rhamnose inducible promoter with the arabinose inducible P_{araB} using standard molecular biology techniques and isothermal assembly (*52*) using the NEB HiFi DNA Assembly Master Mix (New England Biolabs). The resulting *kmR-araBp-ccdB* ("KAC") cassette allowed for efficient counter-selection on LB plates containing 10% arabinose. We also constructed a variant of this cassette with the gentamicin resistance (*gmR-araBp-ccdB* or "GAC").

b. Construction of Cloning Vectors for Transcriptional Reporters

Cloning vectors pMK4 and pMK7 were constructed from pUA66 (*55*). In pMK4, the GFP coding sequence and ribosomal binding site (RBS) of pUA66 were replaced by Venus NB ("VenNB") (*25*) and the RBS of Gene 10 in T7 phage ("T7 RBS") consisting of the sequence TTTAAGAAGGAGATATACAT. In pMK7, the GFP coding sequence and RBS of pUA66 were replaced by SCFP3A (*25*) and the T7 RBS while the kanamycin resistance cassette and the lambda T0 terminator were replaced with an ampicillin resistance cassette and a high-efficiency terminator from the ilvGEDA regulatory region (*66*). In addition, for both pMK4 and pMK7, the original restriction cloning site was replaced with a region flanked by two BsaI recognition sites to allow for insertion of promoter sequences via Golden Gate assembly (*56, 67*). To construct pMK4 and pMK7, linear fragments corresponding to the desired final sequence were prepared either via PCR from pUA66, or generated via custom DNA synthesis as a gBlock® (IDT). These fragments were assembled into a circular plasmid via isothermal assembly using the NEB HiFi DNA Assembly Master Mix (New England Biolabs) following manufacturer protocols.

c. Construction of the Class I Transcriptional Reporter

Unlike most flagellar gene promoters, the regulatory region of the Class I gene FlhDC is highly complex and is sensitive to long range interactions (*53, 68*). To account for these effects, Class I transcription was monitored by a cassette composed of the T7 RBS and VenNB that was directly integrated into the 3' UTR of the endogenous FlhDC transcript. Because the promoter of the neighboring gene MotA resides within the FlhC coding sequence, the codons of FlhC comprising the MotA promoter were replaced with synonymous codons to avoid read-through interference. Both the synonymous mutations and the VenNB insertion were accomplished using the "scarless" technique described above. To confirm that the insertion did not considerably alter downsteam flagellar gene expression, a Class II reporter (fliFp-SCPF3A) was integrated into the GalK locus of this strain and the distribution of CFP fluorescence was compared to that of the same Class II reporter inserted in a wild-type background strain (**fig. S4**).

d. Construction of Strains with Constitutively Expressed FlhDC

We constructed a series of strains where the native Class I promoter, flhDp, was replaced with a

constitutive promoter from a previously described set of synthetic promoters (the "Pro" promoters) (31). Downstream the constitutive promoter, the native RBS for FlhD was replaced with either the T7 RBS or a mutant RBS ("mut4") with the sequence TTTAAGAA**TTGC**ATATACAT (mutated bases in bold). See Table 3 for the list of promoters and RBS used.

Construction of Plasmid Template. An expression cassette containing a Gentamycin resistance cassette and ProB promoter and T7 RBS was ordered from IDT as a gBlock®. A linear fragment consisting of the FlhDC coding sequence was amplified via PCR from MG1655 with primers harboring homologous overhangs to the gBlock and pMK4 plasmid. Finally, a linear fragment consisting of the origin of replication and terminator was amplified from pMK4 plasmid. The three fragments were assembled via isothermal assembly using the NEB HiFi DNA Assembly Master Mix (New England Biolabs). The resulting plasmid, pProB-FlhDC, served as a template for other constitutive promoter-FlhDC constructs. A forward primer that contains mutations that convert ProB into other Pro promoters and a reverse primer whose 5' end meets the 5' end of the forward primer were used to PCR amplify linear DNA from the pProB-FlhDC template. After PCR, the resulting linear fragment (a lineared plasmid with the ProB promoter mutated into the desired Pro promoter) was circularized using the NEB KLD Enzyme Mix (New England Biolabs) according to the manufacturer's protocols. To generate the mut4 plasmids, a ssDNA oligo was designed consisting of the mut4 mutation and flanking regions homologous to FlhD and the Pro promoters. A PCR generated linear fragment comprising the pProB-FlhDC plasmid minus the region consisting of the mut4 specific mutations was assembled with the mut4 oligo via isothermal assembly using the NEB HiFi DNA Assembly Master Mix (New England Biolabs).

Chromosomal Insertion. The Class I reporter strain consisting of VenNB integrated in the 3' region of the FlhDC transcript and the Class II expression reporter fliFp-SCFP3A inserted in the GalK site was used as the parental strain. A linear fragment consisting of an overhang homologous to the 5' end of the flhDp region, selective marker (Gent resistance), Pro promoter, RBS (T7 or mut4) and a fragment of FlhD which served as the second homologous overhang was amplified from each pPro(x)-FlhDC plasmid. This linear fragment was chromosomally inserted via red recombination as described above.

DATA ACQUISITION AND ANALYSIS

a. Microfluidic master fabrication

For our initial experiments, we used an epoxy replica of the "mother machine" described in Potvin-Trottier et al (*24*) (**fig. S1**, Design A). The replica mold was a generous gift from Dr. Matthew Cabeen (Harvard University). Subsequently, we generated custom SU-8 molds to build channels that better matched the typical cell width in our growth conditions. New designs for the microfluidic device were created in AutoCAD; generally, it consists of two layers, one for the cell channels and a second one for the feeding channels. The cell channels were 1.1μm wide and 25μm long. The edges of the channels were smoothed out to reduce the halo that appears during phase-contrast imaging. We also added a trough at the boundary where the cell channels meet the feeding channel so that the phase contrast halo from the feeding channel does not affect the imaging of the cells inside the channel (**fig. S1**, Design B). The feeding channels were 8.1mm long and 100μm wide.

Fabrication of the master mold was carried out using standard UV photolithography in a clean room environment at the Center for Nanoscale Systems at Harvard University. We modified the fabrication procedure from the method described in (*24*) by exposing the SU-8 using a Heidelberg MLA150 Maskless Aligner (Heidelberg Instruments). The MLA150 enabled us to directly "print" our AutoCAD designs without a mask and often resulted in more accurate printing of smaller features.

To print the microfluidic device master, we used the following protocol. The spin coating parameters shown below are written using the abbreviation: speed (rpm)/acceleration (rpm/sec)/time (sec):

1) First layer: cell channels.

    a. Place a 3″ wafer at a spinner and rinse it by adding acetone and isopropyl alcohol (IPA) while it is spinning.
    b. Let the wafer dry for 15 minutes on a hotplate at 200°C.
    c. Let the wafer cool down for a few minutes and place it on a spin chuck.
    d. Slowly pour SU-8 2002 until it covers ~2/3 of the wafer. Here, avoid any bubbles in the resist since even small bubbles can distort the cell channel.
    e. Spin the wafer using the program: Step 1: 500/100/10, Step 2: 3500/300/60.
    f. Bake the wafer for 1 min at 65°C, 1 min at 95°C, 1 min at 65°C.
    g. Expose the wafer with the cell channel design using the MLA150 with a dosage of 2500 mJ/cm^2. In our cell channel design, we also include cross-shaped marks which will serve as alignment marks during the exposure of the feeding channel layer.
    h. After exposure in the MLA, bake the wafer for 1 min at 65°C, 1 min 95°C and 30 seconds at 65°C.
    i. Gently immerse the wafer in a SU-8 developer.
    j. Bake the wafer for 15 minutes on a hot plate at 150°C ("hard bake" step).
    k. Measure the channel height using a profilometer. The expected high is ~1.2μm.

2) Second layer: feeding channels.

    a. Place the wafer with the cell channels on a spin chuck.
    b. Slowly pour SU-8 2010 photoresist on the wafer covering ~2/3 of its area.
    c. Spin the wafer using the program: Step 1: 500/100/10. Step 2: 3000/300/60.
    d. Bake it using hot plates for 1 min at 65°C, 2 min 95°C and 1 min at 65°C.
    e. Use cotton swabs soaked with propylene-glycol-methyl-ether-acetate (PGMA) to wipe SU-8 off from the region of the wafer where the alignment crosses are printed.
    f. Bake the wafer at 65°C for 1 minute.
    g. Load the feeding channel design into the MLA. Place the wafer in the MLA and align the wafer by identifying the crosses using the cameras of the MLA. Once alignment is complete, expose with a dosage of 4500 mJ/cm^2 and focus offset ("defoc") -2.
    h. Once the design is exposed, bake the wafer at 65°C for 1 min, 95°C for 4 min and 65°C for 1 min.
    i. Immerse the wafer in a container with PGMA and shake it very slowly for 1 min.
    j. Rinse the wafer with IPA to remove the remaining SU-8.
    k. Let the wafer hard bake at 150ºC for 15 minutes.
    l. Measure the feeding channel height using the profilometer. The expected height is ~11μm.

b. Cell Segmentation and Tracking

We used custom software in MATLAB based on previously described algorithms (*24*, *61–63*) to analyze time-lapse movies. We used RFP fluorescence as the "reference" image channel for segmentation. Parameters of the segmentation algorithm were empirically optimized for our typical image conditions. Once the "masks" defining individual cells were determined, images from the YFP and CFP data channels were aligned to the RFP segmentation to correct for any mis-registration between the data channels. The horizontal shift between the reference RFP channel and the data channel (YFP & CFP) was computed by taking the horizontal projection of each channel and computing the cross-correlation function using the *xcov* function in MATLAB: the shift between fluorescence channels was estimated by determining the lag value where the maximum cross-correlation coefficient occurs. Similarly, the vertical shift was estimated using a cross-correlation analysis of the vertical projections for each fluorescence

channel. The shift between the fluorescence channels was usually very small (1-2 pixels). However, at large lag values, computationally estimated cross-correlations can occasionally generate large (spurious) correlation values. To avoid this problem, we limited the range of lags being considered to ±5 pixels.

In most cases, the cell at the bottom of the growth channel (i.e. the "mother cell") remained virtually in the same position from frame-to-frame. Potential "cell divisions" events were first identified by sudden decreases in cell area, i.e. if a cell's area dropped to less than 60% of its current value in the next frame. Errors were corrected by manual review. Measurements of mean fluorescence were typically robust to these segmentation errors: erroneous over-segmentation resulted in two symmetric "half-cells" with the same mean fluorescence as the original full size cell while erroneous under-segmentation resulted in fluorescence of two daughter cells being averaged together which, due to the shared parental history, tended to be relatively similar. Each lineage was tracked to the end of the experiment or until the mother cells were "lost" from the channels. For simplicity, only lineages that survived and continued to divide to the end of the experiment were analyzed. In rare occasions, mother cells became filamentous or stopped growing. These lineages were discarded from analysis or tracked only up to the last "normal" cell division.

Once the cells corresponding to the mother cell lineage were identified in each frame, we extracted the mean fluorescence for all three (YFP, CFP and RFP) fluorescence channels and determined the cell length. We computed the mean fluorescence by collecting and averaging the pixel values of the fluorescence image that lie within the mask corresponding to the mother cell. For each mother cell, we also estimated the approximate cell length: due to the vertical (or near-vertical) orientation of the almost all mother cells, the distance between the top- and bottom-most pixels of the mother cell was taken to be reasonable estimates of the cell length.

For the input-output relationship experiments where FlhDC expression was driven by promoters P1-P7 (e.g. Fig. 5 from the main text), cell identification and tracking was supplemented with software designed for automated processing of Mother Machine experiments, named Molyso (*64*). No substantial differences were observed between fluorescence time-lapse traces generated by either software.

c. Time-lapse Data Analysis

i) Estimation of promoter activity

The activity of a promoter driving a transcript expressing a fluorescent protein can be estimated by the amount of new fluorescent protein produced between two time points). The fluorescent proteins used in our experiments are generally very stable and undergo negligible degradation. Under such conditions

$$F_{total}(t) \cong F_{total}(t-1) + P(t)$$

where F_{total} is the total fluorescence of the cell and P(t) is the amount of new fluorescence produced between *t-1* and *t*. Thus, in principle, we could estimate *P* from the change is total fluorescence within the cell between two frames. However, estimation of the total fluorescence is sensitive to exact segmentation of each individual cell. Therefore, we instead opted to use methods of promoter activity estimation based on changes in the mean fluorescence (i.e. the average pixel intensity) in the cell as previously described in (*24*, *65*)**.** Briefly, if the total area of the cell is A(t) and the average pixel intensity

is *C(t)*, then $F_{total} = A(t)C(t)$. It follows that $\frac{dF_{total}}{dt} = C\frac{dA}{dt} + A\frac{dC}{dt}$ which can be rearranged to give

$$\frac{1}{A}\frac{dF_{total}}{dt} = C\frac{1}{A}\frac{dA}{dt} + \frac{dC}{dt}$$

We chose to use the left term $\frac{1}{A}\frac{dF_{total}}{dt}$, i.e. the "cell-size normalized" production rate, as a proxy for promoter activity. Because the transcriptional pulses we observed were extremely large and lasted multiple cell generations, this normalization had a negligible effect while simplifying our promoter activity estimation (**fig. S5**). Operationally, we estimated $\frac{1}{A}\frac{dA}{dt}$, i.e. the relative growth rate of the cell, by taking the log ratio of the initial and final area of the cell for each cell division. We estimated $\frac{dC}{dt}$ by smoothing our fluorescence traces with a Savitzky-Golay filter and taking the numerical derivative.

ii) Estimation of "on" and "off" states

To estimate the duration of "on" and "off" states, we first applied a mild Savitzky-Golay filter to our promoter traces. We then defined a heuristic threshold to identify the "pulse on" and "pulse off" states for each promoter. First, using cells without any fluorophores, we estimated the background "promoter activity" of *E. coli* under our experimental conditions which arises due to autofluorescence. From this measurement, we obtained the mean and standard deviations of autofluorescence-associated background activity. We defined the mean + 2×standard deviation of this background activity as our "low detection threshold". When we applied this threshold to our Class II and Class III promoter activity traces, we discovered that this threshold was too sensitive and that we detected many small "bursts" of transcription lasting under 10 minutes. We hypothesized that those bursts might be "leaky" transcripts that occur even during inactive states. Therefore, we collected all short bursts, lasting 10 minutes or less and computed the mean and standard deviation of those bursts. This process allowed us to define a second threshold as the + 2×standard deviation of "leaky transcript" activity. Time periods when the promoter activity was continuously above this threshold was defined as "on" periods. Similarly, "off" periods were defined as contiguous time periods with promoter values below this threshold.

iii) Input-output relationship between promoters across different classes

To determine the input-output relationship between Class II and Class III, we divided the Class II reporter fluorescence into 5 logarithmically spaced bins that spanned the minimum and maximum Class II fluorescence values measured. We then sorted all observations into these bins based on the Class II fluorescence value. For each bin, we computed the mean observed input (i.e. mean Class II fluorescence) against the mean output (i.e. mean of the paired Class III promoter activity).

We used a similar approach to determine the input-output relationship between Class I and Class II in strains where Class I was driven by different synthetic promoters. However, unlike the Class II reporter, the Class I reporter fluorescence has a much smaller variance (see **fig. S6**) and therefore it was more difficult to distinguish between periods of sustained high fluorescence and short random fluctuations, possibly due to measurement or reporter "noise". To overcome this effect, we binned our time-lapse data into 2 hour windows (corresponding to ~2 cell divisions) and averaged the Class I fluorescence and Class II promoter activity for each time bin. This step effectively allowed us to determine whether the Class I fluorescence and Class II promoter activity was "consistently" high over a given 2 hour time period. We then divided the resulting time-binned Class I reporter values into 5 logarithmically-spaced amplitude-

bins that spanned the minimum and maximum Class I fluorescence values measured. For each bin, we computed the mean input (i.e. mean Class I fluorescence) against the mean of the corresponding output (i.e. Class II promoter activity).

In strains where FlhDC expression is driven by the mut4 RBS, the same number of transcripts produces fewer FlhDC compared to strains with the T7RBS. However, the YFP reporter in these strains has its own RBS and thus only reports the amount of transcript produced. To account for this effect, we constructed a strain with a mut4RBS that had the same level of Class II expression as a strain with a T7RBS. We used this strain to derive a correction factor for Class I YFP fluorescence in mut4 strains (~0.221) so that we could appropriately compare the FlhDC expression levels in mut4 strains relative to the T7RBS strains **(fig. S8).**

IMPACT OF INSERTION ELEMENT MUTATION ON FLAGELLAR TRANSCRIPTION

The heterogeneity in flagellar gene expression appears to contradict previous physiological observations that individual *E. coli* have on average 2-3 flagella during mid-exponential growth (*69-71*). However, strains classically used in chemotaxis studies (such as RP437 or W3110) were found to harbor in insertion element in the regulatory region of *flhDC* (*53*). By contrast, the background strain for this work, MG1655 (CGSC #6300) does not have any insertion elements in this region. Interestingly, we note that unlike CGSC #6300, the original isolate of MG1655 submitted by the Blattner lab to the Coli Genetic Stock Center, MG1655 (seq) (CGSC #7740) which derives from the subculture used by the Blattner lab for the complete genomic sequencing of *E. coli* harbors an IS1 element in the regulatory region of FlhDC (*53*).

To determine whether the apparent difference in flagellar gene regulation might be specifically due to the insertion element mutation, we replaced the native FlhDC regulatory region with a homologous region from W3110 which carries an IS5 insertion. This "IS5" strain of MG1655 began expressing flagellin homogenously at a high level (**fig. S9**). This result supports our hypothesis that the pulsing behavior may have been previously obscured in many common *E. coli* strains that harbor the insertion element.

IMPACT OF CLASS II AND CLASS III GENES ON CLASS II PULSES

In *Salmonella,* two Class II genes were shown to participate in feedback regulation of FlhDC. The Class II gene product FliZ in *Salmonella* acts as a transcriptional repressor for YdiV (*46*). Hence, expression of FliZ leads to increased activation of FlhDC. A second Class II protein FliT was found to directly bind the FlhC subunit of FlhDC and prevent the complex from associating with DNA (*72, 73*). However, FliT was unable to interact with FlhDC that was pre-bound to DNA (*72*).

By contrast, in *E. coli*, we found that neither FliZ nor FliT had a notable effect on heterogeneous Class II gene expression (**fig. S10**). For FliZ, we note that the 5' untranslated region of YdiV in *Salmonella* and *E coli* show considerable divergence: transcription of YdiV in *Salmonella* is thought to be regulated by the neighboring nlpC gene promoter, while its *E. coli* counterpart is thought to be expressed from its own promoter within this region (*32*). Based on our observations, we hypothesized that flagellar pulses in *E. coli* occur without FliZ-YdiV feedback.

To further test this idea, we generated a plasmid pPro3-YdiV where YdiV was expressed from a constitutive promoter Pro3. As described in the main text, a Δ*ydiV* mutation causes Class II genes to become more continuously active, i.e. the pulses to disappear (fig. S11 B). Consequently, the promoter activity distribution becomes narrow compared to the wild-type strain (**fig. S11 D**). When we transformed a Δ*ydiV* mutant strain with pPro3-YdiV, Class II genes began pulsing again, in a manner reminiscent of wild-type strain (**fig. S11 A, C**): the distribution of Class II promoter activity also became

wide again, similar to the wild-type strain (**fig. S11 D**).

To determine whether the pulsatile behavior of the pPro3-YdiV strain was indeed similar to pulses of the wild-type strain, we asked what fraction of pulses initiated at a given point in the cell division cycle. From our time-lapse data, we divided each cell generation into 10 intervals and then calculated what fraction of the pulses initiated within each interval (**fig. S11 E**). This analysis revealed that wild-type flagellar pulses initiated with nearly equal frequency at all points of the cell division cycle and that pPro3-YdiV pulses recapitulated this property. We similarly asked what fraction of pulses terminated at a given point in the cell division cycle (**fig. S11 F**). We again found that wild-type pulses and pPro3-YdiV pulses showed similar distributions across the cell cycle, suggesting that pulses in pPro3-YdiV strains are indeed similar to wild-type pulses.

Having investigated the role of FliZ and FliT in flagellar pulses, we also investigated whether FliA, the sigma factor responsible for Class III activation, could potentially affect Class II pulses via feedback interaction. However, deletion of FliA did not substantially alter the distribution of Class II gene expression (**fig. S10**). Since Class III genes cannot be expressed in Δ*fliA*, by extension we also believe that Class III gene products do not influence Class II pulses.

Finally, we asked whether the flagellar basal body complex could potentially influence Class II pulses. To address this question, we deleted the class II protein FliF which was previously been shown to be necessary for the formation of flagellar basal bodies (*74*). Again, we observed no substantial difference in Class II gene expression in this strain (**fig. S10**) suggesting that Class II pulses occur independently of basal body assembly/inheritance.

COMPARISON WITH BISTABLE FLAGELLAR EXPRESSION IN SALMONELLA

In populations of *Salmonella*, flagellar expression occurs in a bistable manner: for both Class II (e.g. *fliA*) and Class III promoters (e.g. *fliC*), flow cytometry shows a bimodal distribution of gene expression (*18*, *19*, *75*). By contrast, in *E. coli* we observe a wide but unimodal distribution for Class II genes (such as *fliA*, shown in **fig. S3**) when we measure gene expression in culture via flow cytometry (**fig. S12**). Class III genes such as *fliC* show a more bimodal distribution but the distribution corresponding to the "on" state is still considerably more smeared than in *Salmonella.*

What might account for these differences? Comparison between Class II and Class III genes of *E. coli* may offer a clue: as described in our work, Class II genes pulsate at a higher frequency while Class III genes spend a considerably longer period in the "off" state. Thus, we hypothesize that the smearing observed in Class II genes (and in the "on" state of Class III genes) reflects the relatively fast time scale of pulses in *E. coli*. In fact, theoretical work suggests that in a genetic switch that transitions stochastically between "on" and "off" states, the frequency of these transitions determines the shape of the distribution of gene expression within the population: low transition frequencies (i.e. long lived "on" and "off" states) give bimodal distributions, whereas higher transition frequencies lead to wide unimodal distributions (*76*). As a corollary, we hypothesize that flagellar gene expression in *Salmonella* is considerably more stable over time—cells reside in an "on" or "off" state for extended periods of time. This model would also be consistent with the involvement of a feedback loop (FliZ-YdiV), which as discussed above, appears to be non-existent (or non-functional) in *E. coli*.

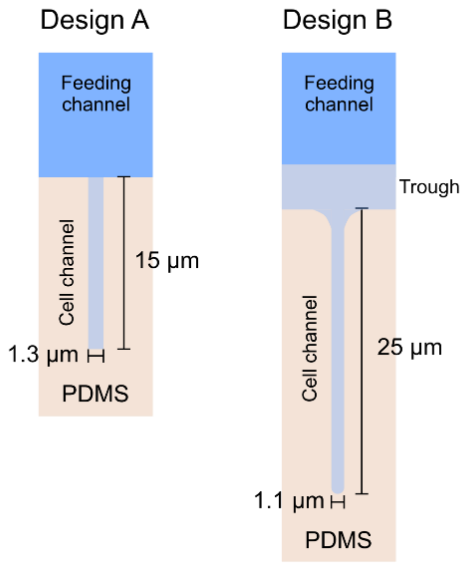

Fig. S1. Schematic of the microfluidic device. (Left) Design A used for initial experiments. This design accommodates ~3-4 cells per cell channel. (Right) Design B incorporates several modifications. The cell channels are thinner (1.1µm vs 1.3µm) and extended to 25µm long to accommodate ~6-8 cells. The narrower channels are better suited for maintaining cells in a vertical orientation under our growth conditions. The edges of the channels are rounded which reduces the halo effect during phase contrast microscopy. Finally, a shallow trough is placed between the cell channel and the feeding channel so that the phase contrast halo from the feeding channel does not interfere with imaging of the cells within the cell channel.

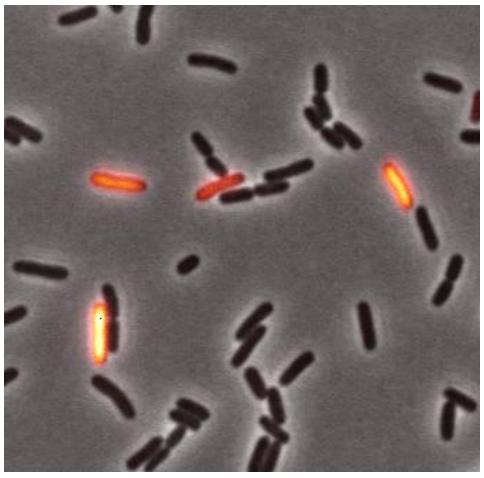

Fig. S2. Flagellar gene expression is heterogeneous when cells are grown in liquid suspension. Example image of cells with a fliCp-YFP reporter grown in liquid culture. Shown is an overlay of phase contrast and YFP fluorescence (orange) images. Cells were grown in liquid culture at 30ºC in the modified Neidhardt EZ rich media with shaking at 250rpm until OD=0.5. 1µl of the culture was then deposited onto an agarose pad (2% w/v, low melting point agarose BP165, Fisher Scientific) and a coverslip was placed on top to allow imaging under the microscope.

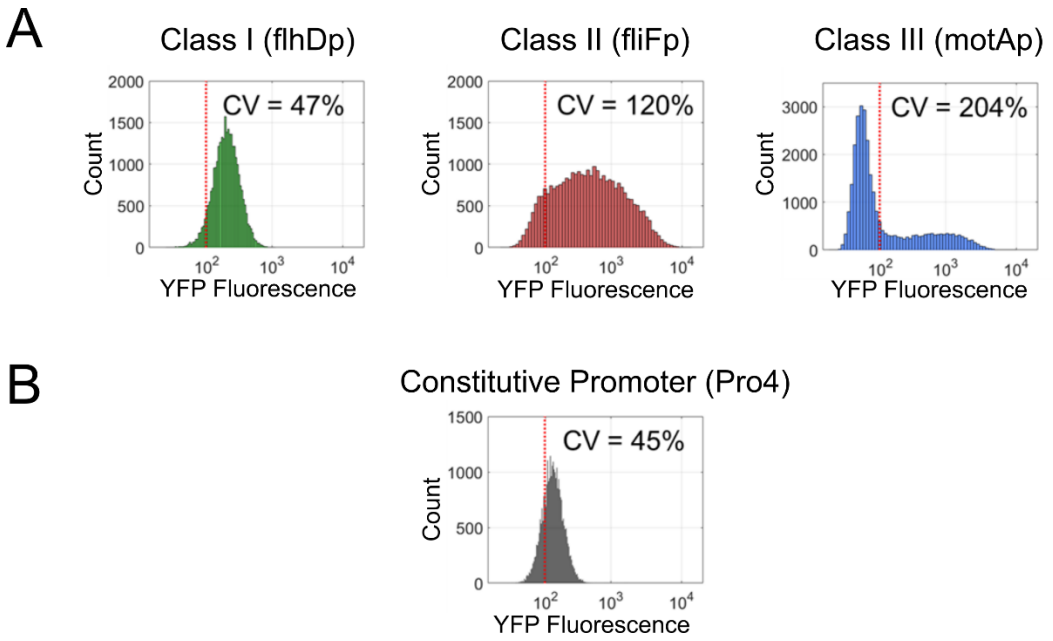

Fig. S3. Flow cytometry analysis of flagellar gene expression for cells grown in liquid culture. (A) Typical fluorescence distribution of Class I, II and III promoter reporters. Shown is the fluorescence distribution of cells harboring the flhD, fliF or motA promoters fused to YFP. Cells were grown in liquid culture and measured via flow cytometry as described above. Coefficient of variation (CV) values are for each fluorescence distribution. Dashed red line indicates threshold for cellular auto-fluorescence defined as the mean+2×standard deviation of flow cytometry signal from cells without any fluorescent reporters. (B) The fluorescence distribution of a constitutive promoter (Pro4) with similar mean expression to the wild-type flhD promoter. CV and dashed lines are as defined in (A).

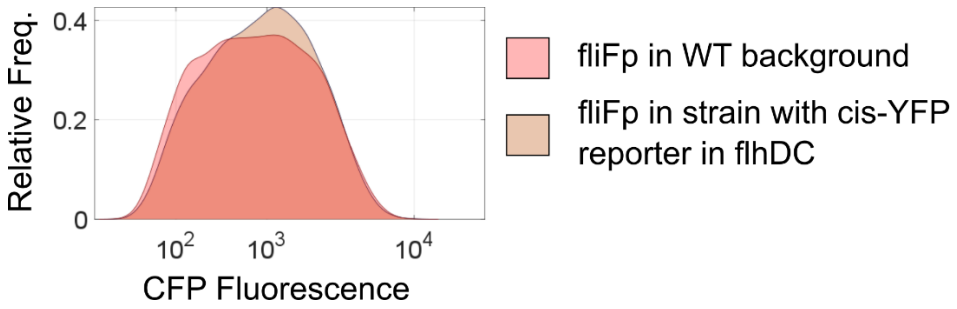

Fig. S4. The cis-YFP reporter in the FlhDC operon does not affect class II gene expression. CFP fluorescence distribution for strains with a Class II (fliF)-CFP reporter with (brown) and without (red) the cis-YFP reporter in FlhDC. Cells were grown in liquid culture and measured via flow cytometry as described in "Growth Conditions". Shown is a kernel density estimate of the fluorescence distribution obtained using the ksdensity function in MATLAB.

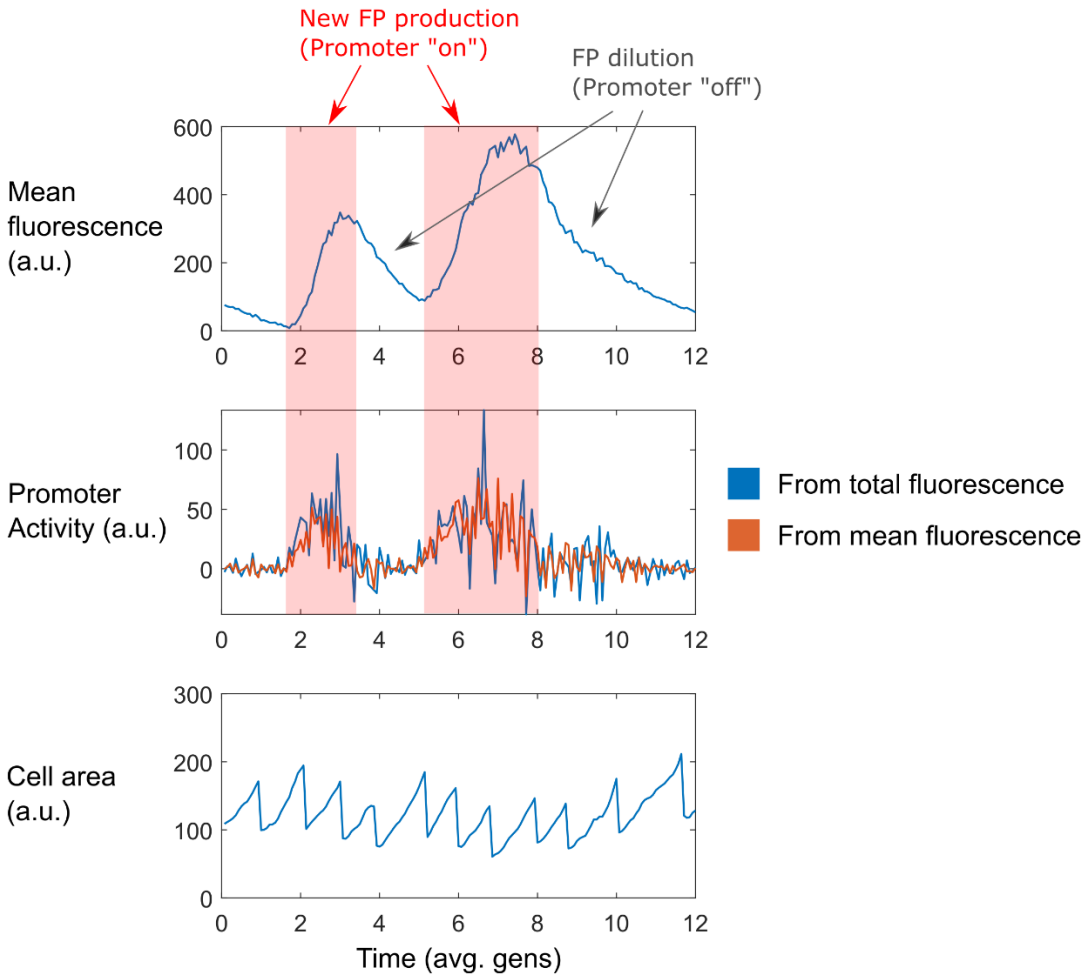

Fig. S5. Estimation of promoter activity from time-lapse data. Example of cell lineage trace from strain with fliFp-CFP reporter. (Top) Mean CFP fluorescence as a function of time. (Middle) Promoter activity estimated using either the total cellular fluorescence (i.e. $P_{abs}(t) = F_{total}(t) - F_{total}(t-1)$, blue trace) or mean cellular fluorescence and growth rate ($P_{rel}(t) = \frac{1}{A}\frac{dF_{total}}{dt} = C\frac{1}{A}\frac{dA}{dt} + \frac{dC}{dt}$, orange trace) as described above in "Estimation of promoter activity". Note that the two methods give different values since $P_{abs}(t) = \frac{1}{A} \times P_{rel}(t)$ but the flagellar gene pulses are largely robust to this difference. Here we show the promoter activity estimated without applying any smoothing on the original fluorescence time-lapse data. In our analyses, we typically apply a mild Savitzky-Golay filter on the raw fluorescence trace to reduce the noise that arises when taking the numerical derivative. (Bottom) Cell area as a function of time. Red shaded region indicates time points where new FPs are created—i.e. when the promoter is "on".

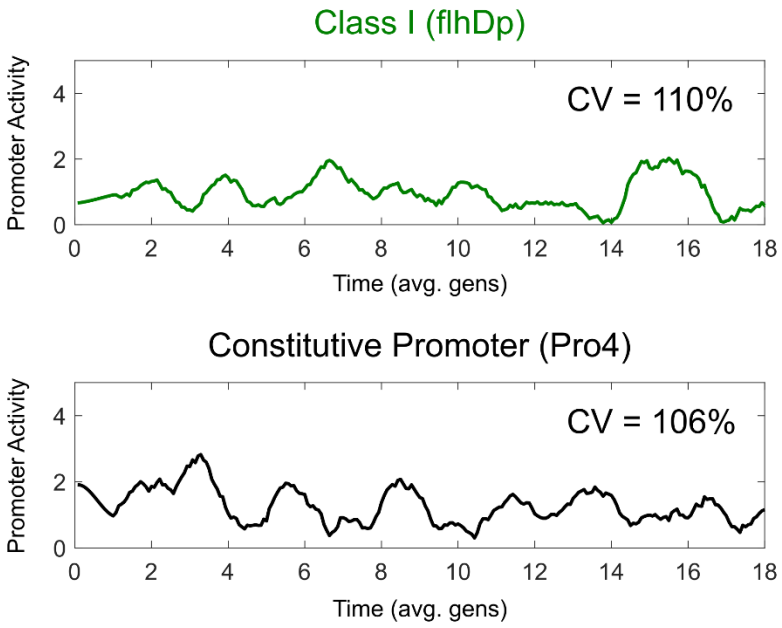

Fig. S6. Class I (flhDp) promoter activity resembles a constitutive promoter. Example of cell lineage trace from strain with flhDp-YFP reporter (top, green) or a constitutive promoter (Pro4-YFP) (bottom, black). The promoter activity traces were normalized by the mean promoter activity of each trace to highlight the variance relative to the mean. The CV value indicates the coefficient of variation for each strain obtained from multiple (n=20) traces.

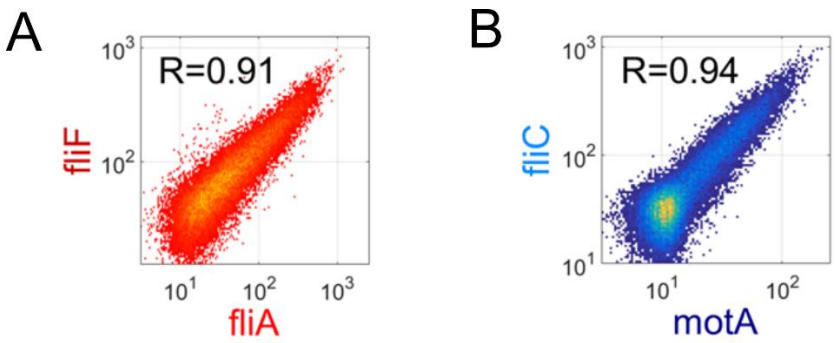

Fig. S7. Promoters within the same class show high correlation. Typical fluorescence distribution in cells harboring two Class II promoter reporters (red) or two Class III promoters (blue), measured via flow cytometry. The R value indicates the Pearson correlation coefficient. (A) A 2D density plot of YFP and CFP fluorescence in cells harboring both fliAp-YFP and fliFp-CFP reporters. (B) A 2D density plot of YFP and CFP fluorescence in cells harboring both motAp-YFP and fliCp-CFP reporters.

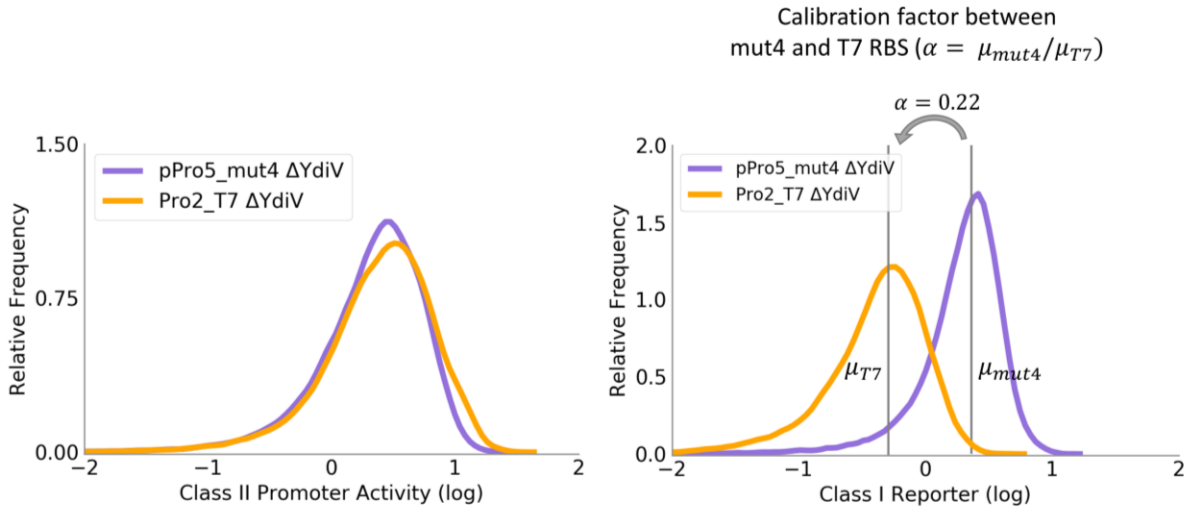

Fig. S8. Calibration of class I reporter for mut4 and T7 RBS. (Left) Distribution of Class II promoter (*fliFp*) activity in a Δ*ydiV* background strain where FlhDC is driven by a Pro5 promoter with a mut4 RBS in a plasmid (purple) and a Pro2 promoter with T7 RBS in the chromosome (orange). (Right) Distribution of Class I reporter (YFP) in the same two strains. Despite having nearly identical Class II activities, the raw Class I reporter signal is considerably different because different RBSs drive FlhDC expression in these two strains. We used these two strains to estimate a "correction factor" between mut4 and T7 RBS strains, using the ratio of the mean Class I reporter levels $\alpha = \mu_{mut4}/\mu_{T7}$= ~0.22. The data was obtained from microfluidic time-lapse experiments.

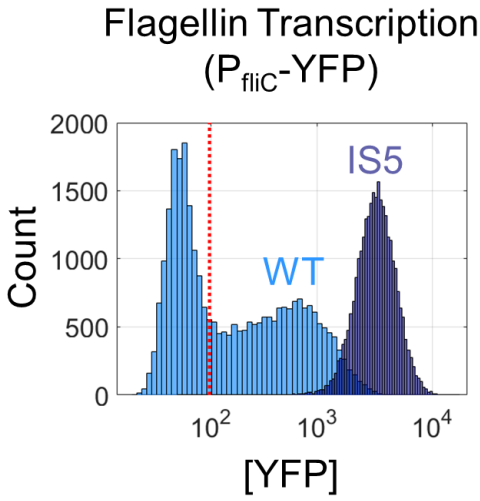

Fig. S9. An insertion element mutation in the FlhDC regulatory region results in high homogenous expression of flagellar genes. Distribution of fluorescence in strains harboring PfliC-YFP reporter with (dark blue) and without (light blue) the insertion element mutation ("IS5"). Fluorescence was measured via flow cytometry. Wild type strains (WT, light blue) show large heterogeneity while insertion element mutants (IS5, dark blue) express flagellin homogeneously. Dashed red line indicates the mean+2σ threshold for cellular auto-fluorescence (as previously described).

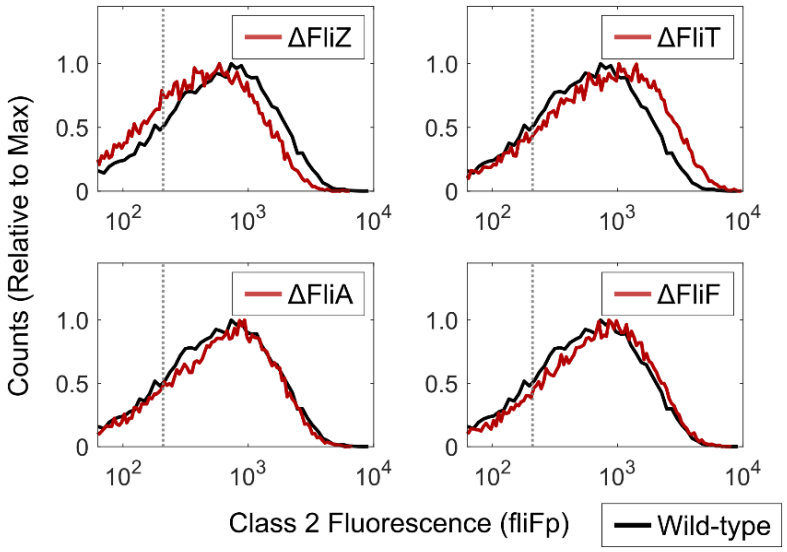

Fig. S10. Effect of flagellar gene deletions on class II pulses. Class II reporter (fliFp) fluorescence distribution for WT (black) and mutants (red). Cells were grown in liquid culture as described above in "GROWTH CONDITIONS", and fluorescence was measured via flow cytometry. In-frame knockouts of the flagellar genes were generated using the techniques described in "Scarless Chromosomal Engineering".

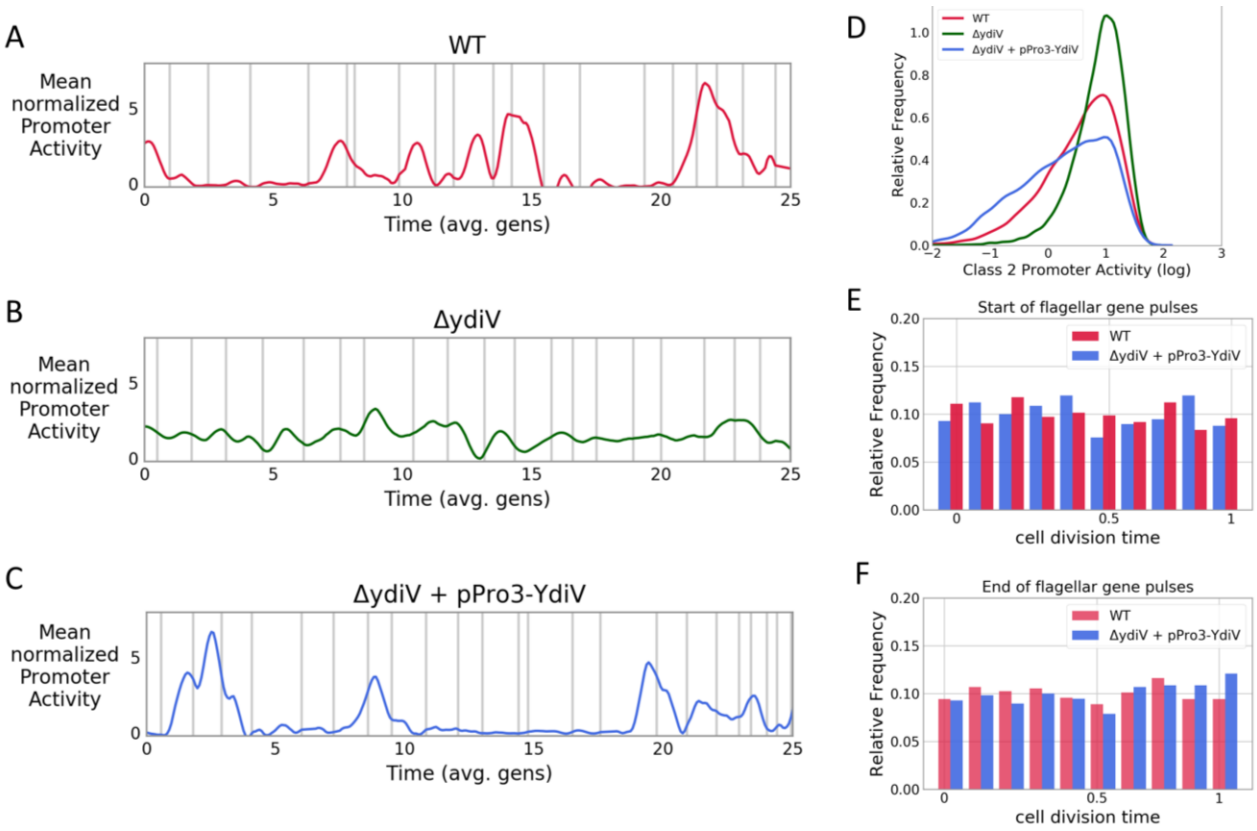

Fig. S11. Constitutively expressed YdiV can restore class II promoter pulses in a ΔydiV mutant of *E. coli.* Representative traces of Class II promoter activity from microfluidic experiments for wild-type (WT) (A), Δ*ydiV* strain (B), and a Δ*ydiV* strain with a plasmid, pPro3-YdiV (C). The gray vertical lines in the time series mark cell division events. (D) Distribution of Class II promoter activity of the three strains (shown in logarithmic scale) for multiple traces (150 per strain) (E) Fraction of observed pulses that initiate at cell division point x for wild-type strain (red) and Δ*ydiV*+pPro3-YdiV (blue). Cell division time is defined as 10 equal size bins and where $x = 0$ is the time interval closest to cell birth and $x = 1$ is the interval before division. (F) Fraction of observed pulses that terminate at cell division point x. Cell division time is as define in (E). Panels E and F suggest that plasmid segregation does not govern the occurrence of the observe pulses because the distribution of pulses along the cell cycle is the same in the presence or absence of plasmids.

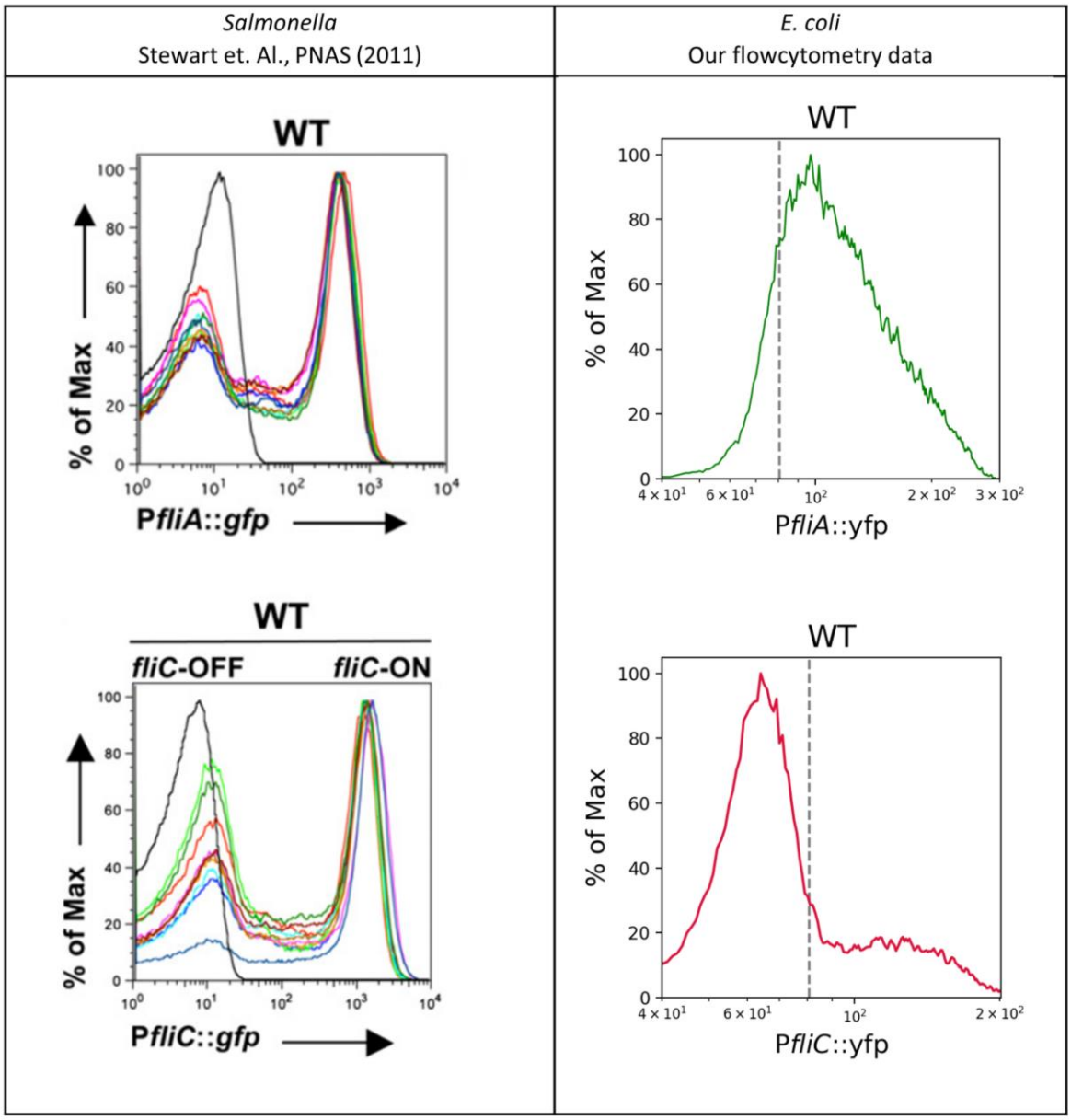

Fig. S12. Comparison of *Salmonella* and *E. coli* class II and III gene expression. In *Salmonella*, expression of Class II promoter P*fliA* and Class III promoter P*fliC* show a clear bimodal distribution (first column, plots reproduced from Stewart et. al (19)). By contrast, the expression of the *E. coli* homologous gene *fliA* shows a unimodal distribution. The *fliC* distribution in *E. coli* shows bimodality but the "on" state is considerably more smeared than in *Salmonella*. The dashed line in the right column indicates the threshold of cellular autofluorescence.

Table 1. List of plasmids.

Plasmid	Source	Antibiotic Marker	Description
pMK4	This work	Kan	Empty vector with YFP (Venus NB)
pMK7	This work	Amp	Empty vector with CFP (SCFP3A)
pMK4-FlgA	This work	Kan	Plasmid containing flgA promoter fused to YFP (Venus NB)
pMK4-FlgB	This work	Kan	Plasmid containing flgB promoter fused to YFP (Venus NB)
pMK4-FlhB	This work	Kan	Plasmid containing flhB promoter fused to YFP (Venus NB)
pMK4-FliA	This work	Kan	Plasmid containing fliA promoter fused to YFP (Venus NB)
pMK4-FliD	This work	Kan	Plasmid containing fliD promoter fused to YFP (Venus NB)
pMK4-FliE	This work	Kan	Plasmid containing fliE promoter fused to YFP (Venus NB)
pMK4-FliF	This work	Kan	Plasmid containing fliF promoter fused to YFP (Venus NB)
pMK4-FliL	This work	Kan	Plasmid containing fliL promoter fused to YFP (Venus NB)
pMK4-FlgK	This work	Kan	Plasmid containing flgK promoter fused to YFP (Venus NB)
pMK4-FlgM	This work	Kan	Plasmid containing flgM promoter fused to YFP (Venus NB)
pMK4-FliC	This work	Kan	Plasmid containing fliC promoter fused to YFP (Venus NB)
pMK4-MotA	This work	Kan	Plasmid containing motA promoter fused to YFP (Venus NB)
pMK4-Tar	This work	Kan	Plasmid containing tar promoter fused to YFP (Venus NB)
pMK7-FliF	This work	Amp	Plasmid containing fliF promoter fused to CFP (SCFP3A)
pMK7-FliC	This work	Amp	Plasmid containing fliC promoter fused to CFP (SCFP3A)
pPro2-FlhDC	This work	Gent	Plasmid containing Pro2 promoter fused to T7 RBS and FlhDC
pPro4-FlhDC	This work	Gent	Plasmid containing Pro4 promoter fused to T7 RBS and FlhDC
pPro5-FlhDC	This work	Gent	Plasmid containing Pro5 promoter fused to T7 RBS and FlhDC
pProB-FlhDC	This work	Gent	Plasmid containing ProB promoter fused to T7 RBS and FlhDC
pProBm4-FlhDC	This work	Gent	Plasmid containing ProB promoter fused to mut4 RBS and FlhDC
pProCm4-FlhDC	This work	Gent	Plasmid containing ProC promoter fused to mut4 RBS and FlhDC
pProDm4-FlhDC	This work	Gent	Plasmid containing ProD promoter fused to mut4 RBS and FlhDC

Plasmid	Source	Antibiotic Marker	Description
pPro5m4-FlhDC	This work	Gent	Plasmid containing Pro5 promoter fused to mut4 RBS and FlhDC
pSIM5	Gift of D. Court	Cm	Helper plasmid encoding red recombinase proteins
pCP20	CGSC	Amp, Cm	Helper plasmid encoding FLP recombinase
pPro3-YdiV	This work	Gent	Plasmid containing Pro3 promoter fused to YdiV

Table 2. List of strains.

Strain	Source	Description
MG1655 (CGSC 6300)	CGSC	Background Strain
MG1655+IS5	This work	See below
MGR	This work	MG1655 IntS::ZeoR-P_{RNA1}-mCherry
MGR-E98K	This work	MGR *motA(E98K)*
MGR-E98K FliF FlhD ("E98KFD")	This work	MGR-E98K galK::AmpR-P_{fliF}-CFP flhDC-YFP (see below)
MGR-E98K FliF FlgA	This work	MGR-E98K galK::AmpR-P_{fliF}-CFP attB::KmR-P_{flgA}-YFP
MGR-E98K FliF FlgB	This work	MGR-E98K galK::AmpR-P_{fliF}-CFP attB::KmR-P_{flgB}-YFP
MGR-E98K FliF FlhB	This work	MGR-E98K galK::AmpR-P_{fliF}-CFP attB::KmR-P_{flhB}-YFP
MGR-E98K FliF FliA	This work	MGR-E98K galK::AmpR-P_{fliF}-CFP attB::KmR-P_{fliA}-YFP
MGR-E98K FliF FliD	This work	MGR-E98K galK::AmpR-P_{fliF}-CFP attB::KmR-P_{fliD}-YFP
MGR-E98K FliF FliE	This work	MGR-E98K galK::AmpR-P_{fliF}-CFP attB::KmR-P_{fliE}-YFP
MGR-E98K FliF FliF	This work	MGR-E98K galK::AmpR-P_{fliF}-CFP attB::KmR-P_{fliF}-YFP
MGR-E98K FliF FliL	This work	MGR-E98K galK::AmpR-P_{fliF}-CFP attB::KmR-P_{fliL}-YFP
MGR-E98K FliF FliC ("E98KFC")	This work	MGR-E98K galK::AmpR-P_{fliF}-CFP attB::KmR-P_{fliC}-YFP
MGR-E98K FliC FlgK	This work	MGR-E98K galK::AmpR-P_{fliC}-CFP attB::KmR-P_{flgK}-YFP
MGR-E98K FliC FlgM	This work	MGR-E98K galK::AmpR-P_{fliC}-CFP attB::KmR-P_{flgM}-YFP
MGR-E98K FliC FliC	This work	MGR-E98K galK::AmpR-P_{fliC}-CFP attB::KmR-P_{fliC}-YFP
MGR-E98K FliC MotA	This work	MGR-E98K galK::AmpR-P_{fliC}-CFP attB::KmR-P_{motA}-YFP
MGR-E98K FliC Tar	This work	MGR-E98K galK::AmpR-P_{fliC}-CFP attB::KmR-P_{tar}-YFP
E98KFD ProB_mut4	This work	MGR-E98K galK::AmpR-P_{fliF}-CFP flhDC-YFP P_{flhD}::GentR-ProB-mut4
E98KFD ProC_mut4	This work	MGR-E98K galK::AmpR-P_{fliF}-CFP flhDC-YFP P_{flhD}::GentR-ProC-mut4
E98KFD Pro2_T7	This work	MGR-E98K galK::AmpR-P_{fliF}-CFP flhDC-YFP P_{flhD}::GentR-Pro2-T7
E98KFD ProD_mut4	This work	MGR-E98K galK::AmpR-P_{fliF}-CFP flhDC-YFP P_{flhD}::GentR-ProD_mut4
E98KFD Pro4_T7	This work	MGR-E98K galK::AmpR-P_{fliF}-CFP flhDC-YFP P_{flhD}::GentR-Pro4-T7
E98KFD Pro5_T7	This work	MGR-E98K galK::AmpR-P_{fliF}-CFP flhDC-YFP P_{flhD}::GentR-Pro5-T7
E98KFD ProB_T7	This work	MGR-E98K galK::AmpR-P_{fliF}-CFP flhDC-YFP P_{flhD}::GentR-ProB-T7
E98KFD ΔydiV	This work	MGR-E98K galK::AmpR-P_{fliF}-CFP flhDC-YFP ydiV::FRT

E98KFC Pro4 ΔflgM	This work	MGR-E98K galK::AmpR-P_{fliF}-CFP flhDC-YFP P_{flhD}::GentR-Pro4 flgM::FRT
E98KFD ProB_mut4 ΔydiV	This work	MGR-E98K galK::AmpR-P_{fliF}-CFP flhDC-YFP P_{flhD}::GentR-ProB_mut4 ydiV::FRT
E98KFD ProC_mut4 ΔydiV	This work	MGR-E98K galK::AmpR-P_{fliF}-CFP flhDC-YFP P_{flhD}::GentR-ProC-mut4 ydiV::FRT
E98KFD Pro2_T7 ΔydiV	This work	MGR-E98K galK::AmpR-P_{fliF}-CFP flhDC-YFP P_{flhD}::GentR-Pro2-T7 ydiV::FRT
E98KFD ProD_mut4 ΔydiV	This work	MGR-E98K galK::AmpR-P_{fliF}-CFP flhDC-YFP P_{flhD}::GentR-ProD-mut4 ydiV::FRT
E98KFD Pro4_T7 ΔydiV	This work	MGR-E98K galK::AmpR-P_{fliF}-CFP flhDC-YFP P_{flhD}::GentR-Pro4-T7 ydiV::FRT
E98KFD Pro5_T7 ΔydiV	This work	MGR-E98K galK::AmpR-P_{fliF}-CFP flhDC-YFP P_{flhD}::GentR-Pro5-T7 ydiV::FRT
E98KFD ProB_T7 ΔydiV	This work	MGR-E98K galK::AmpR-P_{fliF}-CFP flhDC-YFP P_{flhD}::GentR-ProB-T7 ydiV::FRT
E98KFD ΔydiV pPro3-YdiV	This work	MGR-E98K galK::AmpR-P_{fliF}-CFP flhDC-YFP ydiV::FRT pPro3-YdiV
E98KFC+IS5	This work	MGR-E98K+IS5 galK::AmpR-P_{fliF}-CFP attB::KmR-P_{fliC}-YFP

Table 3. List of the combination of promoter and RBS used to control class I expression and the notation used in this work to reference them.

Class I Promoter_RBS	Promoter Label
ProB_mut4	P1
ProC_mut4	P2
Pro2_T7	P3
ProD_mut4	P4
Pro4_T7	P5
Pro5_T7	P6
ProB_T7	P7